

Node-to-node method for planar frictionless contact problems with small deformation

Kun Wang

2020.05.02-2020.05.07

1 Geometry

A body \mathcal{B} is regarded as a set of points in a region of the Euclidean space \mathbb{E}^3 . The position of a point in the reference configuration is denoted as $\mathbf{X} \in \mathbb{E}^3$. The deformed configuration of a body \mathcal{B} is a one-to-one mapping $\phi_t : \mathcal{B} \rightarrow \mathbb{E}^3$ which places the body to a new region. The subscript t indicates the configuration at the instant t . The position of the corresponding point in the deformed configuration, also called the current configuration, is referred to as \mathbf{x} and

$$\mathbf{x} = \phi_t(\mathbf{X}) = \phi(\mathbf{X}, t). \quad (1)$$

The contact pair includes two bodies, \mathcal{B}_1 and \mathcal{B}_2 , which are illustrated in fig. 1. \mathbf{x}^1 and \mathbf{x}^2 respectively are candidate contact points on the two bodies. \mathbf{n}^1 is the normal to the contact surface of the body \mathcal{B}_1 .

The gap between the two candidate contact points is defined as

$$g_n = (\mathbf{x}^2 - \mathbf{x}^1)^T \mathbf{n}^1 \quad (2)$$

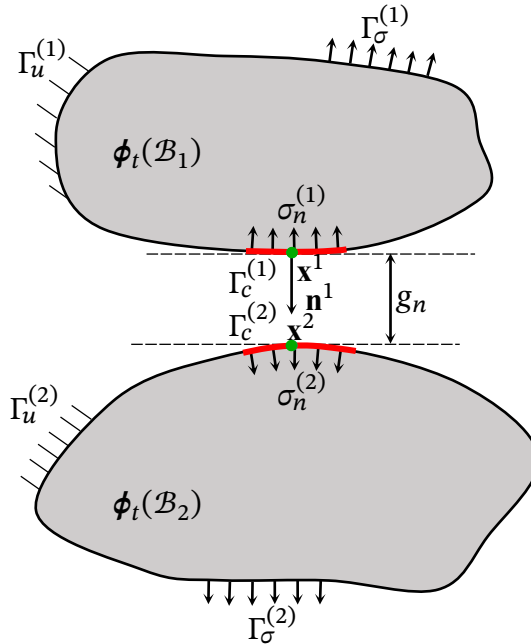


Figure 1: The geometry of two contact bodies

2 Contact conditions

For the case of the normal contact, the two bodies should not penetrate each other, which means the gap function should not be negative,

$$g_n = (\mathbf{x}^2 - \mathbf{x}^1)^T \mathbf{n}^1 \geq 0 \quad (3)$$

3 Equilibrium equations

The strong form

$$\begin{aligned} \nabla \boldsymbol{\sigma} + \mathbf{f}_b - \rho \ddot{\mathbf{u}} &= \mathbf{0} & \text{in } \Omega \\ \boldsymbol{\sigma} \mathbf{n} &= \mathbf{t}_\sigma & \text{in } \Gamma_\sigma \\ \mathbf{u} &= \mathbf{u}_0 & \text{in } \Gamma_u \\ g_n(\mathbf{x}) &\geq 0 & \text{in } \Gamma_c \end{aligned} \quad (4)$$

where $\boldsymbol{\sigma}$ is the Cauchy stress tensor. \mathbf{f}_b is the body force. \mathbf{u} is the displacement vector and \mathbf{n} is the normal vector of the boundary. \mathbf{t}_σ is the pressure on the boundary. The first equation in Eq. (4) is derived at the current configuration so it is suitable for all the systems with small deformations or with large deformations.

4 Weak form

According to the well-known *principle of virtual work*, the weak form of the equilibrium equations without contact contributions is derived as follows.

$$\int_{\Omega} (\nabla \boldsymbol{\sigma} + \mathbf{f}_b - \rho \ddot{\mathbf{u}}) dv \delta \mathbf{u} - \int_{\Gamma_\sigma} (\boldsymbol{\sigma} \mathbf{n} - \mathbf{t}_\sigma) \delta \mathbf{u} ds = 0 \quad (5)$$

According to the Gauss divergence theorem, one can obtain

$$\begin{aligned} \int_{\Gamma_\sigma} (\boldsymbol{\sigma}^T \mathbf{n})^T \delta \mathbf{u} ds &= \int_{\Gamma_\sigma} (\boldsymbol{\sigma} \delta \mathbf{u})^T \mathbf{n} ds = \int_{\Omega} \nabla (\boldsymbol{\sigma} \delta \mathbf{u}) dv \\ &= \int_{\Omega} (\nabla \boldsymbol{\sigma}) \delta \mathbf{u} + \boldsymbol{\sigma} : \frac{\partial (\delta \mathbf{u})}{\partial \mathbf{x}} dv = \int_{\Omega} (\nabla \boldsymbol{\sigma}) \delta \mathbf{u} + \boldsymbol{\sigma} : (\delta \mathbf{F}) \mathbf{F}^{-1} dv \end{aligned} \quad (6)$$

Substituting eq. (6) into eq. (5) yeilds

$$\int_{\Omega} (\mathbf{f}_b - \rho \ddot{\mathbf{u}}) dv \delta \mathbf{u} - \int_{\Omega} \boldsymbol{\sigma} : (\delta \mathbf{F}) \mathbf{F}^{-1} dv + \int_{\Gamma_\sigma} \mathbf{t}_\sigma \delta \mathbf{u} ds = 0. \quad (7)$$

In eq. (7), the Cauchy stress $\boldsymbol{\sigma}$ is not associated with the Cauchy-Green strain. The stress tensor associated with the Cauchy-Green strain is the second Piola-Kirchhoff (PK2) stress tensor

$$\boldsymbol{\sigma}_{PK2} = J \mathbf{F}^{-1} \boldsymbol{\sigma} (\mathbf{F}^{-1})^T. \quad (8)$$

Substituting the Cauchy stress tensor with the PK2 stress tensor yeilds

$$\int_{\Omega} (\mathbf{f}_b - \rho \ddot{\mathbf{u}}) dv \delta \mathbf{u} - \int_{\Omega} \boldsymbol{\sigma}_{PK2} : \delta \boldsymbol{\varepsilon} dv + \int_{\Gamma_\sigma} \mathbf{t}_\sigma \delta \mathbf{u} ds = 0. \quad (9)$$

The frictionless contact cotribution of different methods are listed as follows.

Lagrange multiplier method

$$\int_{\Omega} (\mathbf{f}_b - \rho \ddot{\mathbf{u}}) dv \delta \mathbf{u} - \int_{\Omega} \boldsymbol{\sigma}_{PK2} : \delta \boldsymbol{\varepsilon} dv + \int_{\Gamma_{\sigma}} \mathbf{t}_{\sigma} \delta \mathbf{u} ds + \int_{\Gamma_c} (\delta \lambda_N g_N + \lambda_N \delta g_N) ds = 0 \quad (10)$$

Penalty method

$$\int_{\Omega} (\mathbf{f}_b - \rho \ddot{\mathbf{u}}) dv \delta \mathbf{u} - \int_{\Omega} \boldsymbol{\sigma}_{PK2} : \delta \boldsymbol{\varepsilon} dv + \int_{\Gamma_{\sigma}} \mathbf{t}_{\sigma} \delta \mathbf{u} ds + \int_{\Gamma_c} k g_n \delta g_n ds = 0 \quad (11)$$

5 Discretization

The contact bodies and the contact interfaces all need to be discretized to reduce the eq. (4) of the continuum system to an equation with finite degree of freedom (DOF). The continuous bodies are discretized with the well-known finite element method (FEM). To discretize the contact interface, several methods, such as node-to-node (NTN) method, node-to-segment (NTS) method and segment-to-segment (STS) method, have been developed[2]. In this section, the bilinear quadrilateral element will be introduced for planar problems with small deformations. The discretization of the contact interface is implemented by the NTN method. It's worth noting that the NTN method is only valid for *matching* meshes. The introduction of it is just for study.

5.1 Discretization of bodies

The bilinear quadrilateral elements [5, 6] are used for discretizing planar bodies. The displacement field of a finite element is

$$\mathbf{u} = \mathbf{S} \mathbf{q}^e = \begin{bmatrix} \mathbf{N}_1 & \mathbf{N}_2 & \mathbf{N}_3 & \mathbf{N}_4 \end{bmatrix} \mathbf{q}^e \quad (12)$$

where

$$\mathbf{q}^e = \begin{bmatrix} \mathbf{q}_1 \\ \mathbf{q}_2 \\ \mathbf{q}_3 \\ \mathbf{q}_4 \end{bmatrix} \quad (13)$$

$$\mathbf{q}_i = \begin{bmatrix} u_i \\ v_i \end{bmatrix} \quad (14)$$

$$\begin{aligned} N_1 &= \frac{1}{4} (1 - \xi) (1 - \eta) \\ N_2 &= \frac{1}{4} (1 + \xi) (1 - \eta) \\ N_3 &= \frac{1}{4} (1 + \xi) (1 + \eta) \\ N_4 &= \frac{1}{4} (1 - \xi) (1 + \eta) \end{aligned} \quad (15)$$

$$\mathbf{x} = \sum_{i=1}^4 N_i \mathbf{x}_i \quad (16)$$

$$\mathbf{u} = \sum_{i=1}^4 N_i \mathbf{u}_i \quad (17)$$

$$\begin{aligned} x &= \sum_{i=1}^4 N_i x_i \\ y &= \sum_{i=1}^4 N_i y_i \end{aligned} \quad (18)$$

$$\begin{aligned} u &= \sum_{i=1}^4 N_i u_i \\ v &= \sum_{i=1}^4 N_i v_i \end{aligned} \quad (19)$$

$$\begin{aligned} \frac{\partial N_1}{\partial \xi} &= \frac{\eta - 1}{4}, \quad \frac{\partial N_2}{\partial \xi} = \frac{1 - \eta}{4}, \quad \frac{\partial N_3}{\partial \xi} = \frac{1 + \eta}{4}, \quad \frac{\partial N_4}{\partial \xi} = -\frac{\eta + 1}{4} \\ \frac{\partial N_1}{\partial \eta} &= \frac{\xi - 1}{4}, \quad \frac{\partial N_2}{\partial \eta} = -\frac{1 + \xi}{4}, \quad \frac{\partial N_3}{\partial \eta} = \frac{1 + \xi}{4}, \quad \frac{\partial N_4}{\partial \eta} = \frac{1 - \xi}{4} \end{aligned} \quad (20)$$

$$\frac{\partial x}{\partial \xi} = \sum_{i=1}^4 \frac{\partial N_i}{\partial \xi} x_i, \quad \frac{\partial x}{\partial \eta} = \sum_{i=1}^4 \frac{\partial N_i}{\partial \eta} x_i \quad (21)$$

$$\begin{aligned} \varepsilon_x &= \frac{\partial u}{\partial x} \\ \varepsilon_y &= \frac{\partial v}{\partial y} \\ \gamma_{xy} &= \frac{\partial u}{\partial y} + \frac{\partial v}{\partial x} \end{aligned} \quad (22)$$

$$\frac{\partial \mathbf{u}}{\partial \mathbf{x}} = \frac{\partial \mathbf{u}}{\partial \boldsymbol{\xi}} \left(\frac{\partial \mathbf{x}}{\partial \boldsymbol{\xi}} \right)^{-1} = \begin{bmatrix} \frac{\partial u}{\partial x} & \frac{\partial u}{\partial y} \\ \frac{\partial v}{\partial x} & \frac{\partial v}{\partial y} \end{bmatrix} = \begin{bmatrix} \frac{\partial u}{\partial \xi} & \frac{\partial u}{\partial \eta} \\ \frac{\partial v}{\partial \xi} & \frac{\partial v}{\partial \eta} \end{bmatrix} \begin{bmatrix} \frac{\partial x}{\partial \xi} & \frac{\partial x}{\partial \eta} \\ \frac{\partial y}{\partial \xi} & \frac{\partial y}{\partial \eta} \end{bmatrix}^{-1} = \frac{1}{|J|} \begin{bmatrix} \frac{\partial u}{\partial \xi} & \frac{\partial u}{\partial \eta} \\ \frac{\partial v}{\partial \xi} & \frac{\partial v}{\partial \eta} \end{bmatrix} \begin{bmatrix} \frac{\partial y}{\partial \eta} & -\frac{\partial x}{\partial \eta} \\ -\frac{\partial y}{\partial \xi} & \frac{\partial x}{\partial \xi} \end{bmatrix} \quad (23)$$

$$J = \begin{bmatrix} \frac{\partial x}{\partial \xi} & \frac{\partial x}{\partial \eta} \\ \frac{\partial y}{\partial \xi} & \frac{\partial y}{\partial \eta} \end{bmatrix} \quad (24)$$

$$\begin{aligned} \varepsilon_x &= \frac{1}{|J|} \left(\frac{\partial u}{\partial \xi} \frac{\partial y}{\partial \eta} - \frac{\partial u}{\partial \eta} \frac{\partial y}{\partial \xi} \right) = \frac{1}{|J|} \left[\left(\sum_{i=1}^4 \frac{\partial N_i}{\partial \xi} u_i \right) \left(\sum_{i=1}^4 \frac{\partial N_i}{\partial \eta} y_i \right) - \left(\sum_{i=1}^4 \frac{\partial N_i}{\partial \eta} u_i \right) \left(\sum_{i=1}^4 \frac{\partial N_i}{\partial \xi} y_i \right) \right] \\ \varepsilon_y &= \frac{1}{|J|} \left(\frac{\partial v}{\partial \eta} \frac{\partial x}{\partial \xi} - \frac{\partial v}{\partial \xi} \frac{\partial x}{\partial \eta} \right) = \frac{1}{|J|} \left[\left(\sum_{i=1}^4 \frac{\partial N_i}{\partial \eta} v_i \right) \left(\sum_{i=1}^4 \frac{\partial N_i}{\partial \xi} x_i \right) - \left(\sum_{i=1}^4 \frac{\partial N_i}{\partial \xi} v_i \right) \left(\sum_{i=1}^4 \frac{\partial N_i}{\partial \eta} x_i \right) \right] \\ \gamma_{xy} &= \frac{1}{|J|} \left(-\frac{\partial u}{\partial \xi} \frac{\partial x}{\partial \eta} + \frac{\partial u}{\partial \eta} \frac{\partial x}{\partial \xi} + \frac{\partial v}{\partial \xi} \frac{\partial y}{\partial \eta} - \frac{\partial v}{\partial \eta} \frac{\partial y}{\partial \xi} \right) \\ &= \frac{1}{|J|} \left[-\left(\sum_{i=1}^4 \frac{\partial N_i}{\partial \xi} u_i \right) \left(\sum_{i=1}^4 \frac{\partial N_i}{\partial \eta} x_i \right) + \left(\sum_{i=1}^4 \frac{\partial N_i}{\partial \eta} u_i \right) \left(\sum_{i=1}^4 \frac{\partial N_i}{\partial \xi} x_i \right) \right. \\ &\quad \left. + \left(\sum_{i=1}^4 \frac{\partial N_i}{\partial \xi} v_i \right) \left(\sum_{i=1}^4 \frac{\partial N_i}{\partial \eta} y_i \right) - \left(\sum_{i=1}^4 \frac{\partial N_i}{\partial \eta} v_i \right) \left(\sum_{i=1}^4 \frac{\partial N_i}{\partial \xi} y_i \right) \right] \end{aligned} \quad (25)$$

$$\begin{aligned}
 \varepsilon_x &= \frac{1}{|J|} \left(\frac{\partial u}{\partial \xi} \frac{\partial y}{\partial \eta} - \frac{\partial u}{\partial \eta} \frac{\partial y}{\partial \xi} \right) = \frac{1}{|J|} \left[a \left(\sum_{i=1}^4 \frac{\partial N_i}{\partial \xi} u_i \right) - b \left(\sum_{i=1}^4 \frac{\partial N_i}{\partial \eta} u_i \right) \right] \\
 \varepsilon_y &= \frac{1}{|J|} \left(\frac{\partial v}{\partial \eta} \frac{\partial x}{\partial \xi} - \frac{\partial v}{\partial \xi} \frac{\partial x}{\partial \eta} \right) = \frac{1}{|J|} \left[c \left(\sum_{i=1}^4 \frac{\partial N_i}{\partial \eta} v_i \right) - d \left(\sum_{i=1}^4 \frac{\partial N_i}{\partial \xi} v_i \right) \right] \\
 \gamma_{xy} &= \frac{1}{|J|} \left(-\frac{\partial u}{\partial \xi} \frac{\partial x}{\partial \eta} + \frac{\partial u}{\partial \eta} \frac{\partial x}{\partial \xi} + \frac{\partial v}{\partial \xi} \frac{\partial y}{\partial \eta} - \frac{\partial v}{\partial \eta} \frac{\partial y}{\partial \xi} \right) \\
 &= \frac{1}{|J|} \left[-d \left(\sum_{i=1}^4 \frac{\partial N_i}{\partial \xi} u_i \right) + c \left(\sum_{i=1}^4 \frac{\partial N_i}{\partial \eta} u_i \right) + a \left(\sum_{i=1}^4 \frac{\partial N_i}{\partial \xi} v_i \right) - b \left(\sum_{i=1}^4 \frac{\partial N_i}{\partial \eta} v_i \right) \right]
 \end{aligned} \tag{26}$$

where

$$\begin{aligned}
 a &= \sum_{i=1}^4 \frac{\partial N_i}{\partial \eta} y_i \\
 b &= \sum_{i=1}^4 \frac{\partial N_i}{\partial \xi} y_i \\
 c &= \sum_{i=1}^4 \frac{\partial N_i}{\partial \xi} x_i \\
 d &= \sum_{i=1}^4 \frac{\partial N_i}{\partial \eta} x_i
 \end{aligned} \tag{27}$$

$$\begin{bmatrix} \varepsilon_x \\ \varepsilon_y \\ \gamma_{xy} \end{bmatrix} = \mathbf{B} \mathbf{u} \tag{28}$$

$$\mathbf{B} = \frac{1}{|J|} [\mathbf{B}_1 \quad \mathbf{B}_2 \quad \mathbf{B}_3 \quad \mathbf{B}_4] \tag{29}$$

$$\mathbf{B}_i = \begin{bmatrix} a \frac{\partial N_i}{\partial \xi} - b \frac{\partial N_i}{\partial \eta} & 0 \\ 0 & c \frac{\partial N_i}{\partial \eta} - d \frac{\partial N_i}{\partial \xi} \\ c \frac{\partial N_i}{\partial \eta} - d \frac{\partial N_i}{\partial \xi} & a \frac{\partial N_i}{\partial \xi} - b \frac{\partial N_i}{\partial \eta} \end{bmatrix} \tag{30}$$

Planar, small deformation

$$\delta U = -t \int_{\Omega} (\delta \boldsymbol{\varepsilon})^T \boldsymbol{\sigma} dx dy = -t \int_{\Omega} (\delta \mathbf{q}^e)^T \mathbf{B}^T \mathbf{D} \mathbf{B} \mathbf{q}^e dx dy = -(\delta \mathbf{q}^e)^T t \int_{\Omega} \mathbf{B}^T \mathbf{D} \mathbf{B} dx dy \mathbf{q}^e \tag{31}$$

where $\boldsymbol{\varepsilon} = [\varepsilon_x \quad \varepsilon_y \quad \gamma_{xy}]^T$, $\boldsymbol{\sigma} = [\sigma_x \quad \sigma_y \quad \tau_{xy}]^T$, \mathbf{D} is the constitutive matrix. For the case of plane stress,

$$\mathbf{D} = \frac{E}{1-\nu^2} \begin{bmatrix} 1 & \nu & 0 \\ \nu & 1 & 0 \\ 0 & 0 & \frac{1-\nu}{2} \end{bmatrix} \tag{32}$$

For the case of plane strain,

$$\mathbf{D} = \frac{E}{(1-\nu)(1-2\nu)} \begin{bmatrix} 1-\nu & \nu & 0 \\ \nu & 1-\nu & 0 \\ 0 & 0 & \frac{1-2\nu}{2} \end{bmatrix} \tag{33}$$

where E is the Young's modulus and ν is the Lamé factor.

For simplicity, the stiffness matrix is defined as

$$\mathbf{K} = t \int_{\Omega} \mathbf{B}^T \mathbf{D} \mathbf{B} dx dy = t \int_{-1}^1 \int_{-1}^1 \mathbf{B}^T \mathbf{D} \mathbf{B} |J| d\xi d\eta \quad (34)$$

where t is the thickness.

Other integrals in eq. (9) after the discretization are listed as follows.

$$\int_{\Omega} (\delta \mathbf{u})^T \ddot{\mathbf{u}} \rho t dA = (\delta \mathbf{q}^e)^T \int_{\Omega} t \rho \mathbf{S}^T \mathbf{S} dA \ddot{\mathbf{q}}^e = (\delta \mathbf{q}^e)^T \mathbf{M}^e \ddot{\mathbf{q}}^e \quad (35)$$

$$\int_{\Omega} (\delta \mathbf{u})^T \mathbf{f}_b t dA = (\delta \mathbf{q}^e)^T \int_{\Omega} t \mathbf{S}^T \mathbf{f}_b dA = (\delta \mathbf{q}^e)^T \mathbf{Q}_b^e \quad (36)$$

$$\int_{\Gamma_{\sigma}} (\delta \mathbf{u})^T \mathbf{t}_{\sigma} t dL = (\delta \mathbf{q}^e)^T \int_{\Gamma} t \mathbf{S}^T \mathbf{t}_{\sigma} dL = (\delta \mathbf{q}^e)^T \mathbf{Q}_s^e \quad (37)$$

5.2 Discretization of the contact interfaces

The node-to-node approach is introduced to discretize the contact interface. The contact between the two discretized bodies is illustrated in fig. 2.

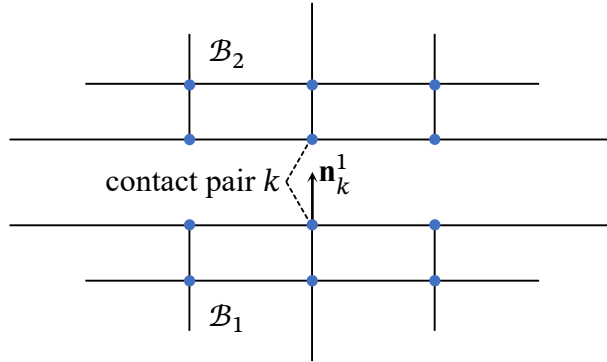


Figure 2: The NTN contact between two discretized bodies

The gap function is redefined as

$$g_n^k = \mathbf{n}_k^1{}^T (\mathbf{u}_k^2 - \mathbf{u}_k^1) \quad (38)$$

5.2.1 Node-to-node contact

Lagrange multiplier method The contact contribution in the virtual work is [2] (Section 8.2, P.189)

$$\int_{\Gamma_c} (\delta \lambda_n g_n + \lambda_n \delta g_n) dA = t \sum_{k=1}^{n_A} (\delta \lambda_n^k g_n^k + \lambda_n^k \delta g_n^k) L_k, \quad (39)$$

where n_A is the number of active contact pairs. With

$$\delta g_n^k = \mathbf{n}_k^1{}^T (\delta \mathbf{u}_k^2 - \delta \mathbf{u}_k^1), \quad (40)$$

eq. (39) can be written as follows.

$$\begin{aligned}
 \int_{\Gamma_c} (\delta\lambda_n g_n + \lambda_n \delta g_n) dA &= t \sum_{k=1}^{n_A} \left(\delta\lambda_n^k \begin{bmatrix} -\mathbf{n}_k^1 & \mathbf{n}_k^1 \end{bmatrix}^T \begin{bmatrix} \mathbf{u}_k^1 \\ \mathbf{u}_k^2 \end{bmatrix} + \lambda_n^k \begin{bmatrix} \delta\mathbf{u}_k^1 \\ \delta\mathbf{u}_k^2 \end{bmatrix}^T \begin{bmatrix} -\mathbf{n}_k^1 \\ \mathbf{n}_k^1 \end{bmatrix} \right) L_k \\
 &= \sum_{k=1}^{n_A} \begin{bmatrix} \delta\mathbf{u}_k^1 \\ \delta\mathbf{u}_k^2 \\ \delta\lambda_n^k \end{bmatrix}^T t L_k \begin{bmatrix} \mathbf{0} & \mathbf{0} & -\mathbf{n}_k^1 \\ \mathbf{0} & \mathbf{0} & \mathbf{n}_k^1 \\ -\mathbf{n}_k^1 & \mathbf{n}_k^1 & \mathbf{0} \end{bmatrix} \begin{bmatrix} \mathbf{u}_k^1 \\ \mathbf{u}_k^2 \\ \lambda_n^k \end{bmatrix} \\
 &= \sum_{k=1}^{n_A} \begin{bmatrix} \delta\mathbf{u}_k^1 \\ \delta\mathbf{u}_k^2 \\ \delta\lambda_n^k \end{bmatrix}^T \mathbf{K}_c \begin{bmatrix} \mathbf{u}_k^1 \\ \mathbf{u}_k^2 \\ \lambda_n^k \end{bmatrix}
 \end{aligned} \tag{41}$$

Penalty method The contact contribution in the virtual work is [2] (Section 8.2, P.190)

$$\int_{\Gamma_c} \epsilon g_n \delta g_n dA = t \epsilon \sum_{k=1}^{n_A} g_n^k \delta g_n^k L_k, \tag{42}$$

where ϵ is the penalty parameter. Substituting eq. (40) into eq. (42) yeilds

$$\int_{\Gamma_c} \epsilon g_n \delta g_n dA = \sum_{k=1}^{n_A} \begin{bmatrix} \delta\mathbf{u}_k^1 \\ \delta\mathbf{u}_k^2 \end{bmatrix}^T t L_k \epsilon \begin{bmatrix} -\mathbf{n}_k^1 \\ \mathbf{n}_k^1 \end{bmatrix} \begin{bmatrix} -\mathbf{n}_k^1 & \mathbf{n}_k^1 \end{bmatrix}^T \begin{bmatrix} \mathbf{u}_k^1 \\ \mathbf{u}_k^2 \end{bmatrix} L_k = \sum_{k=1}^{n_A} \begin{bmatrix} \delta\mathbf{u}_k^1 \\ \delta\mathbf{u}_k^2 \end{bmatrix}^T \mathbf{K}_c \begin{bmatrix} \mathbf{u}_k^1 \\ \mathbf{u}_k^2 \end{bmatrix} \tag{43}$$

6 Results

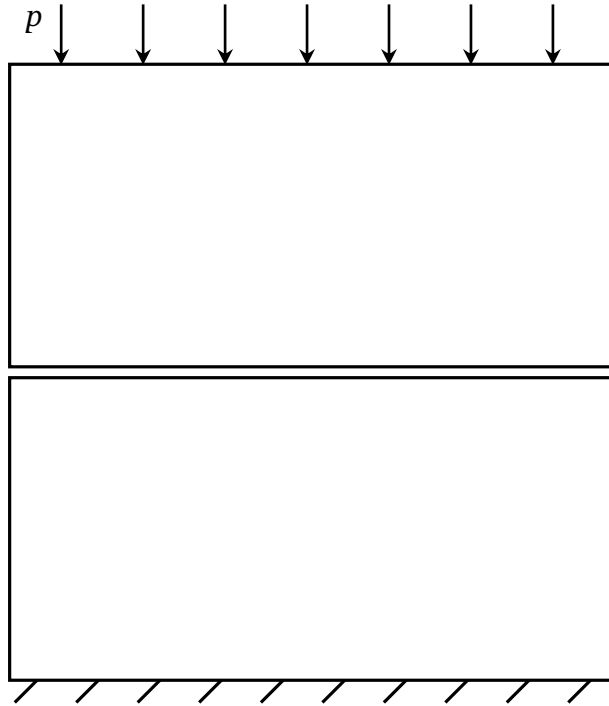


Figure 3: The contact model of two planar plates

The contact model of the two planar plates are illustrated as fig. 3. The two plates have same parameters. The length and the width of the two plates respectively are 1m and 0.5m. The thickness is $t = 0.1\text{m}$. Young's modulus $E = 210\text{GPa}$ and $\nu = 0$. Both two plates are meshed with 10×10 grids.

The magnitude of the pressure load is $p = 1\text{MPa}$. The penalty parameter is $\varepsilon = 10^8$. The bottom side of the upper plate initially coincides with the top side of the lower plate. The gap shown in fig. 3 is just for demonstrating that they are two plates instead of one.

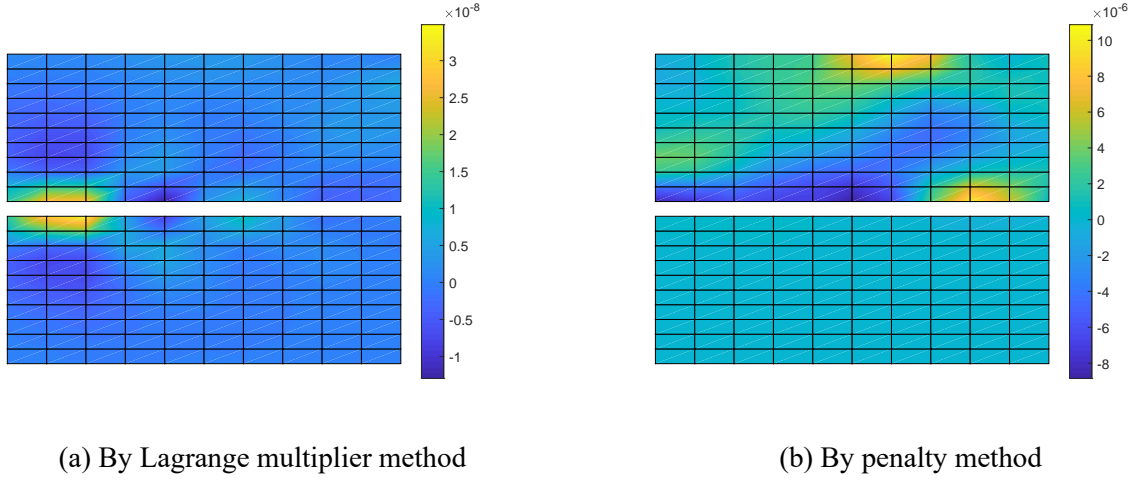


Figure 4: σ_x

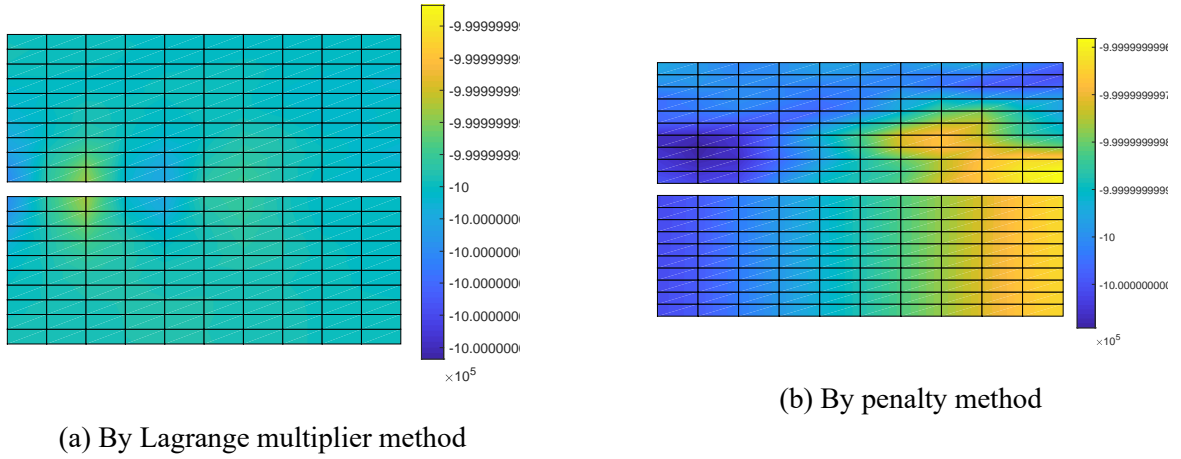


Figure 5: σ_y

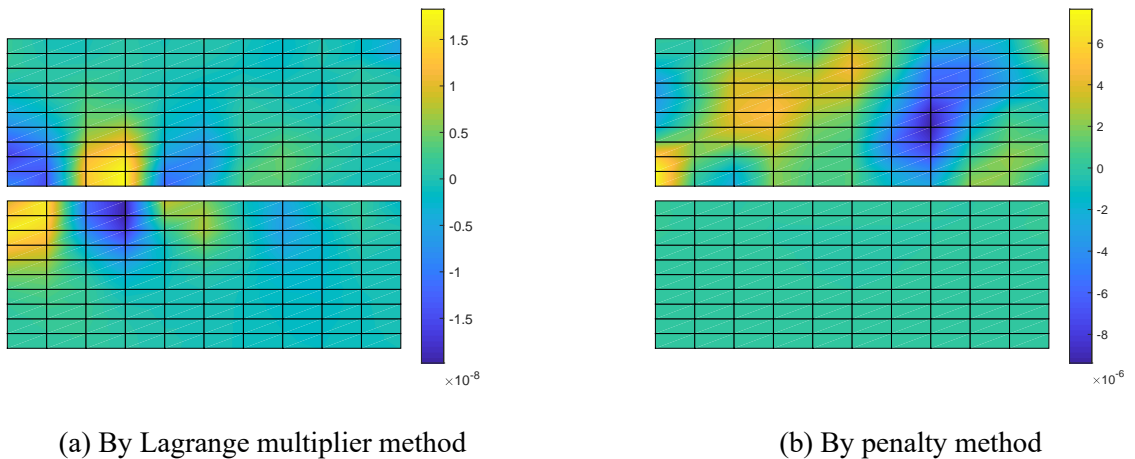


Figure 6: τ_{xy}

In this example, $\nu = 0$ means that the deformation of the two plates should be equal to the result of an uniaxial compression, namely, $\sigma_x = 0$, $\sigma_y = -1\text{MPa}$ and $\tau_{xy} = 0$. fig. 4-6, show that the results from the Lagrange multiplier method and the penalty method are very close to the analytical solutions and the Lagrange multiplier method possess higher accuracy than the penalty method.

References

- [1] A.A. Shabana Computational Continuum Mechanics, 3rd Edition, John Wiley & Sons, Ltd., 2018.
- [2] Wriggers P. Computational Contact Mechanics, 2nd edition. Springer, Berlin, Heidelberg, New York, 2006.
- [3] J.C., Simo, T.A. Laursen, An augmented lagrangian treatment of contact problems involving friction, Computers & Structures, 42(1):97-116.1992.
- [4] V.A. Yastrebov, Numerical Methods in Contact Mechanics, John Wiley & Sons, Ltd. 2013.
- [5] P.I. Kattan, MATLAB Guide to Finite Elements, 2nd edition, Springer, Berlin, Heidelberg, NewYork, 2007.
- [6] O.C. Zienkiewicz, R.L. Taylor, The Finite Element Method, Butterworth, Oxford. UK, 2000.